

UNCLASSIFIED

AD 414095

DEFENSE DOCUMENTATION CENTER

FOR

SCIENTIFIC AND TECHNICAL INFORMATION

CAMERON STATION, ALEXANDRIA, VIRGINIA



UNCLASSIFIED

NOTICE: When government or other drawings, specifications or other data are used for any purpose other than in connection with a definitely related government procurement operation, the U. S. Government thereby incurs no responsibility, nor any obligation whatsoever; and the fact that the Government may have formulated, furnished, or in any way supplied the said drawings, specifications, or other data is not to be regarded by implication or otherwise as in any manner licensing the holder or any other person or corporation, or conveying any rights or permission to manufacture, use or sell any patented invention that may in any way be related thereto.

RADC-TDR-63-292

CATALOGED BY DDC

AS AD NO. 414095

TECHNICAL NOTE
ON
HIGH POWER MICROWAVE ELECTRONICS

by

John W. E. Griemsmann

Polytechnic Institute of Brooklyn
Microwave Research Institute
55 Johnson Street
Brooklyn 1, New York

Report PIBMRI-1170-63

Contract No. AF-30(602)-2135

June 10, 1963

414095

MRI

POLYTECHNIC INSTITUTE OF BROOKLYN
MICROWAVE RESEARCH INSTITUTE
DEPARTMENT OF ELECTROPHYSICS

RADC-TDR-63-292

Report No. PIBMRI-1170-63
Contract No. AF-30(602)-2135

TECHNICAL NOTE
ON
HIGH POWER MICROWAVE ELECTRONICS

by
John W. E. Griemsmann

Polytechnic Institute of Brooklyn
Microwave Research Institute
55 Johnson Street
Brooklyn 1, New York

Report PIBMRI-1170-63
Contract No. AF-30(602)-2135

June 10, 1963

Title Page
Abstract
Foreword
Table of Contents
List of Figures
13 Pages of Text
27 Pages of Figures


J. W. E. Griemsmann
Professor

Prepared for
Rome Air Development Center
Research and Technology Division
Air Force Systems Command
United States Air Force
Griffiss Air Force Base
Rome, New York

ABSTRACT

The work progress since the last Technical Note is summarized. Included is a report on the present status of the C-band microwave high power facility located at the Long Island Graduate Center of the Polytechnic Institute of Brooklyn; the design and construction of a high power microwave flywheel operating in oversized rectangular waveguide; the development of two different broadband, gaseous discharge type, C-band microwave switches of low insertion loss and high speed, acting in a few tens of nanoseconds or less and capable of handling megawatt peak powers; and work on the interaction of high microwave fields with metals.

The switching work was aimed toward solving the problem of discharging the energy that will be built up in the microwave flywheel as a short pulse of extremely high power (35-50 Mw). One device is a dc triggered spark gap operating at atmospheric pressure or higher; the other is a waveguide low-pressure hydrogen gas thyatron.

The interaction of high microwave fields with metals was obtained in a coaxial resonator operating in the TE_{01} circular electric mode with the test specimen as inner conductor. With moderate average powers (about 400 w) it was possible to melt thin-walled tubes of stainless steel and aluminum and to simulate the effect that might be produced by a uniform plane wave of several hundred thousand w/cm^2 power density incident (normally) on a sheet of metal.

PUBLICATION REVIEW

This report has been reviewed and is approved.

Approved:

Arthur J. Frohlich
for L. T. C. (USAF)
ARTHUR J. FROHLICH
Chief, Techniques Laboratory
Directorate of Aerospace Surveillance & Control

Approved:

William T. Pope
for L. T. C. (USAF)
WILLIAM T. POPE
Acting Director
Director of Aerospace
Surveillance & Control

FOREWORD

The work contained in this report was sponsored by the Rome Air Development Center, Air Force Systems Command, Griffiss Air Force Base, Rome, New York under Contract No. AF-30(602)-2135.

TABLE OF CONTENTS

	<u>Page</u>
Foreword	
Abstract	
I. Introduction	1
II. High Power Microwave Facility	2
III. Power Enhancement Devices and Related Work	3
A. Traveling Wave Microwave Flywheel	3
B. Theoretical Breakdown Field for Septated Waveguide	4
C. Effect of Beam Voltage Ripple in High Power Pulsed Klystron Amplifier on Resonator Gain	5
D. High Power Switching Devices	6
1. Waveguide Hydrogen Thyatron	6
2. DC Triggered Microwave Spark Gap Switch	8
IV. Interaction of High Microwave Fields with Metals	11

LIST OF FIGURES

- FIG. 1. Oversized High Power C-Band Resonant Ring
2. Multi-deck Feeding Coupler Assembly Showing Flared Transitions
Multi-deck Sampling Coupler Assembly
Partial Layout of Oversized Traveling Wave Resonator
View of Multi-deck Feeding Coupler Showing Coupling Hole Arrays
3. Plot of Electric Field and Equipotentials for Septated Waveguide
4. Relation Between Beam Voltage on Klystron Amplifier and
Relative Phase Shift Between Input and Output Signals
5. Block Diagram of Setup for Measurement of Phase Shift as
Function of Beam Voltage
6. Graphical Plot of Top of Beam Voltage Pulse
7. Chief Spectral Components of Phase-Modulated Klystron Output
Produced by Beam Voltage Pulse of Fig. 6
8. Exploded View - Microwave Low Pressure Gas Discharge Switch Tube
9. Low Pressure Gas Switch
10. Photograph of Waveguide Thyratron Switch
11. Schematic of Modulator
12. Typical Thyratron Switch Tube Waveforms
13. High Power Test Facility
14. Oscillograms of RF Switching
15. Swayback Waveguide Spark Switch
16. Modified Spark Gap Configuration
17. Swayback Waveguide Spark Switch with Hybrid Coupler
18. Pulse Forms Shown on Oscilloscope
19. Test Switching Arrangement
- 20a. Truncated Cone Microwave Spark Gap with Iris
- 20b. Schematic of DC Triggered Microwave Spark Gap
21. Oscillograms of Switching by DC Triggered Microwave Spark
22. Test Arrangement for DC Triggered Microwave Spark
23. Coaxial Cavity
24. Percent of Total Power Dissipated in the Center Conductor of
Coaxial Line Cavity vs. b/a
25. Microwave Test Circuit
26. Power Relationships During Test
27. Fracture of Aluminum Center Conductor (Surface Shows Signs
of Having Been Molten)

I. Introduction

This report summarizes the work accomplishment since the Technical Note on High Power Microwave Electronics, Report PIBMRI-947-61. It describes:

- (1) the present status of the C-band high microwave power facility
- (2) progress on the high power microwave flywheel (traveling wave resonator)
- (3) work on several fast, low loss, high power gas discharge switching devices which promise a solution to the problem of extracting the power out of the flywheel
- (4) experiments recently completed on the interaction of high microwave fields with metals.

Included also are the results of two analyses related to the operation of the flywheel. In one of these, the enhancement of the microwave electric field at the rounded edge of a thin septum in a rectangular waveguide is examined. From the results, the theoretical breakdown strength of septated waveguide, such as is used in mode filters and directional coupler structures, can be inferred. In the second, the effects of phase variation of the klystron amplifier supplying pulsed power to the flywheel are examined with respect to the microwave power build-up in the ring. Such a phase variation can be caused by a small ripple on the pulsed beam voltage of the klystron and it is important to know what effects are to be expected.

II. High Power Microwave Facility:

Prof. S. W. Rosenthal; E. Grimza, E. Malloy

This facility includes a number of high power C-band microwave sources of varying capabilities and suitable for a variety of experimental purposes. These have been described in the previous Technical Note. The one megawatt C-band magnetron system has proved very useful and much work on high power switch testing and interaction of high microwave fields with metals has been accomplished with its aid. The one megawatt rating has, however, been nominal rather than actual because of somewhat improper matching of the modulator pulse forming network impedance to the magnetron and the not quite correct turns ratio of the pulse transformer. This will be corrected in the near future so that the full megawatt peak power output may be realized. The C-band (Sperry SAC 214) klystron system has been operated at about 1.5 megawatts peak, 0.8 microsecond pulse width using a magnetron driver of 20 kw peak power capability. This system, however, is limited at present by the fixed frequency and narrow pulse width of its driver. Procurement of a driver of variable frequency and pulse width with sufficient rf output to enable the klystron amplifier to attain its rated output would greatly enhance the usefulness of that source. The 10 megawatt peak power C-band klystron system is now in full operation and is producing its rated output, but has not yet been completely checked out. It has been used in connection with high power testing of microwave switches and other components, plasma investigations, and in an unusual experiment in which high microwave power was focussed on a hypersonic shock wave.

III. Power Enhancement Devices and Related Work:

Profs. H. Farber, J. W. E. Griemsmann, S. W. Rosenthal,
M. Sucher; H. Goldie, D. Jacenko, M. Klinger; E. Malloy

A. Traveling Wave Microwave Flywheel

The dischargeable traveling wave resonator (TWF) as a peak power enhancement device was fully discussed in the previous Technical Note. Since then, a C-band tall waveguide prototype resonator capable of enhancing an input power of 5 Mw to about 50 Mw has been almost completed. This ring will be only 40 feet long instead of 500 feet as originally contemplated, but will incorporate the same critical components that would have gone into the longer ring and will be expandable to a greater length by simply adding straight oversized waveguide runs. It should be possible to achieve higher simulated power levels with this device than with the longer ring because of the lower losses and to conduct switching experiments at high power levels.

Such a ring will also permit the study of higher mode problems, although the mode resonances will not be nearly so closely spaced as in the longer ring. Nevertheless, such a resonator should yield valuable information with regard to coupling into and out of the ring and with respect to breakdown of mode filters and septated waveguides used in the construction.

A schematic of the ring is shown in Fig. 1 and photographs of the completed components in Fig. 2. The input and output couplers are of a multideck construction and connected to the rest of the ring by curvilinear tapered transitions. Septated modal filters are introduced into the ring between the straight sections of the oversized waveguide to reduce (if not entirely to eliminate) the number of higher modes excited in the oversized ring components. Power will be fed into the input coupler of the ring by means of a tapered transition. The straight portion of the ring will consist of four sections of oversized waveguide each 34" long and having inside dimensions of 5.75" x 11.168". The input coupler will be a multideck device consisting of twelve C-band 11 db sidewall multi-hole directional couplers arranged one on top of the other. This construction should enable the input coupler to handle power twelve times higher than an ordinary C-band directional coupler and also should eliminate the possibility of exciting higher modes in the coupling region where they might give unpredictable results. Losses of the multideck coupler should be almost equal to the losses of the ordinary C-band directional coupler because the power will be divided equally among the parallel waveguides comprising it.

The output or monitoring coupler is similar to the input coupler and consists of a twelve C-band waveguide multideck array. It incorporates, in its construction, two bends which serve to connect the two straight waveguide sections together and thereby close the ring. Power can be coupled out of two of the twelve stages of the coupler into standard C-band waveguide separately. This arrangement permits the simultaneous use of both couplers, each with a different degree of coupling, simplifying, therefore, the study of the performance of the resonant ring under different conditions.

The particular curvilinear shape used in the transitions consists of the arcs of two equal circles of large radius inverted with respect to each other at the midpoint of the transition. (This configuration has been tried in a previous project at our laboratory and proved satisfactory with respect to reducing the generation of higher modes.)

B. Theoretical Breakdown Field for Septated Waveguide

Since septated waveguide is used in the ring resonator both for mode filtering and in the multideck directional coupler assembly, it is important to know the extent to which the breakdown strength is lowered as a result of the corners at the edge of the septum. A theoretical analysis of the electric field enhancement at a suitably rounded corner has been made by means of a conformal mapping technique using a static approximation and the results are given in a table below.

A simple problem was chosen - that of two plane parallel plates of infinite extent, spaced a distance $2a$ apart, containing a third parallel plate (or septum) of semi-infinite extent half way between the two plates and of thickness $2d$, as shown in Fig. 3(a). If the upper and lower plates are at potentials ϕ_3 and ϕ_1 , respectively, there will be an essentially uniform electric field, $E'_\infty = (\phi_3 - \phi_1)/2a$, between the plates far from the edge of the septum. As the septum is approached, the field will be intensified, reaching a maximum value (E'_{\max}) at the edge of the septum, while far from the edge, in the region between the septum and either of the two plates, the field will again become uniform. The latter field is designated as E_∞ and equals $(\phi_3 - \phi_1)/2a(1 - \rho)$, where $\rho = \frac{d}{a}$, or $E_\infty = E'_\infty/(1 - \rho)$. (See Fig. 3(b), which shows the traces of the equipotential surfaces and the field lines for the region between the plane of symmetry, at an intermediate potential $\phi_2 = \phi_1 + (\phi_3 - \phi_1)/2$, and the lower plate.) The assumption has been made that the edge of the septum has been rounded to have (approximately) a semi-circular contour, with radius of curvature equal to d . For an infinitely thin septum, $E'_{\max} = E'_\infty(1 + 2/\pi)$ or $1.637 E'_\infty$, $E_\infty = E'_\infty$. As the septum thickness increases, E'_{\max}/E'_∞ likewise increases as shown in the table below. The complete data for the solution of this problem are given in Appendix A of the Seventh Quarterly Letter Report for the period ending December 31, 1961.

If, instead of a semicircular contour, a semi-elliptical one had been fitted, the field intensification would have been less, the amount of decrease depending on the flatness of the ellipse (semi-major axis parallel to septum). To obtain such a contour, in practice, might, however, be quite difficult.

TABLE - Field Intensification at Rounded Edge of Septum
for Various Radii of Curvature

$\rho = \frac{d}{a}$	0	0.01	0.02	0.05	0.1	0.2	0.3	0.5
$\frac{E_{\max}}{E_{\infty}}$	1.637	1.628	1.620	1.596	1.554	1.471	1.385	1.212
$\frac{E_{\max}}{E'_{\infty}}$	1.637	1.644	1.653	1.680	1.727	1.839	1.979	2.424

C. Effect of Beam Voltage Ripple in High Power Pulsed Klystron Amplifier on Resonator Gain

In the operation of the high power pulsed klystron amplifier supplying the input microwave pulse to the traveling wave resonator, a small ripple occurs in the pulsed beam voltage. Since a variation in beam voltage produces a phase shift in the microwave output of the tube, it was important to examine the effect of the voltage ripple on the gain of the ring resonator. In the analysis that was made*, the phase shift of the amplified signal was calculated as a function of the beam voltage and these results were then applied to the particular waveform of the ripple appearing in the beam voltage.

Theory indicates that the relative phase shift between output and input signal of the klystron amplifier should be an almost linear function of beam voltage (approximately 10 degrees for a one percent change at 150 kv, or 6.7 degrees per kilovolt). This was computed from small signal theory and is shown in the curve designated "ideal" in Fig. 4. Curve 1 in the same figure was experimentally obtained at an rf input power level sufficient to drive the tube to saturation at each value of beam voltage used; curve 2 was experimentally obtained at an rf input level equal to one tenth the value needed for saturation. All three lines have essentially the same slope. The experimental setup for these measurements is shown in block diagram form in Fig. 5. The observed waveform of the beam voltage pulse is shown in Fig. 6. There are two main ripple frequency components present, one due to the sawtooth top, having a 100 kc fundamental component,

*Salvatore Barbasso, Jr., "The Effects of Phase Shift Upon Ring Resonator Performance", Master's Thesis, Department of Electrophysics, Polytechnic Institute of Brooklyn, Long Island Graduate Center, Farmingdale, N.Y., June, 1963.

the other due to the 500 kc ripple riding on the sawtooth. The resulting phase modulation produces sidebands deviating by 100 and 500 kc from the carrier with relative amplitudes as shown in Fig. 7. (The energy of outlying sidebands is negligible.) As a result, the carrier component is reduced to 0.974 of the amplitude for a perfectly flat voltage pulse and the consequent reduction in gain is about 5 percent.

D. High Power Switching Devices

Work has been concentrated on two different types of gas discharge switches giving promise of possessing the necessary qualifications for use with the proposed microwave flywheel. These qualifications are: high switching speed (less than 30 nanoseconds), low insertion loss (less than 0.2db), and high peak and average power handling capability (about 5 megawatts peak, 5 kilowatts average). Both types of switches, in their present state of development, satisfy the first two requirements and are well on their way toward satisfying the third. The first device to be described is a waveguide grid-controlled low pressure gas discharge tube (waveguide hydrogen thyatron). The second is a (high pressure) waveguide microwave spark gap in which the rf discharge is triggered by a high dc field of fast rise time superimposed on the rf field.

1. Waveguide Hydrogen Thyatron

A comprehensive description of the development of this switch has already been prepared as a special report*. Therefore, a brief summary of its construction, principle of operation, and present state of development will be given here.

The construction of this tube is apparent from Figs. 8 and 9; a photograph of the tube is shown in Fig. 10. The tube is a gas triode containing a heated cathode, anode, and a control grid which initiates the discharge. The cathode and anode structures are mounted immediately outside the broad walls of a section of RG-49/U waveguide which is sealed off at each end by a broadband triple iris glass microwave window. The broad walls of the waveguide, suitably perforated, act as the control grid. The tube can be filled with hydrogen from a heated reservoir included in the cathode structure and the gas pressure can be controlled by means of the voltage applied to the reservoir heater.

The grid is normally at negative potential with respect to the cathode and, in this condition, prevents the thermoionically emitted electrons from entering the waveguide region and causing either a microwave or dc discharge. When a positive pulse is applied to the grid (with the anode at a high positive potential), the low pressure hydrogen gas filling the waveguide is rapidly ionized. The resulting high density of

*H. Goldie, "A Fast Broadband High-Power Microwave Switch", Report PIBMRI 1111-63, 11 February 1963, RADC-TDR-63-139.

electrons causes the ionized gas to acquire a negative permittivity and raises the cut-off frequency of the discharge region in the waveguide well above the applied rf frequency. Consequently, the incident rf power is largely reflected, while a small fraction is absorbed in supporting the discharge and an almost negligible amount is permitted to leak past the discharge region.

A block diagram of the charging and discharging circuits for the tube is shown in Fig. 11(a) and a schematic of the modulator in Fig. 11(b). The circuitry is conventional and contains a variable dc power supply, producing up to several kv, a charging choke, hold-off diode, and a pulse forming network (at present this is in the form of several hundred feet of 50 ohm coaxial cable) which is terminated in a resistive load in series with the waveguide thyatron. The load resistance (R_L) is usually, but not necessarily, matched to the cable characteristic impedance Z_0 . When $R_L = Z_0$, the cable will charge up to twice the dc voltage output E_{bb} of the power supply. For $R_L < Z_0$, the cable charges up to a higher voltage*. When the grid of the thyatron is triggered with a positive pulse, the cable discharges through the tube and load resistance, producing a rectangular current pulse whose duration is essentially twice the delay time of the cable. The hold-off diode serves to prevent the discharge of the cable through the power supply. Typical switching waveforms are shown in Fig. 12 and a block diagram of the complete setup used in testing the tube in Fig. 13.

The switch data are summarized below.

The rf switching characteristics are:

peak rf hold-off power	in excess of one megawatt (at 1μ s pulse width)
rf switching time	20-30 nanoseconds
isolation	greater than 40 db
arc loss	0.5 - 0.9 db
"cold" insertion loss	0.1 to 0.2 db
frequency band	limited only by waveguide windows - essentially the entire operating band of RG-49/U waveguide
deionization time	approximately 35μ s

Typical dc operating characteristics are:

forward anode voltage	4 kv
peak anode current	10 - 20 amps
voltage drop across tube when conducting	150 v
grid trigger pulse	50 - 100 v (positive)
pulse repetition rate	500 pps
hydrogen gas pressure	less than 0.2 mm Hg for high rf peak powers

*R.F. Reintjes and G.T. Coate, editors, Principles of Radar, M.I. T. Radar School Staff, Third Edition, pp. 170-176, McGraw-Hill Book Co., N.Y., 1952

Fig. 14 shows a set of oscillograms of the switching action of the tube in which the envelopes of the reflected and transmitted rf pulse are compared on a dual beam oscilloscope under three different conditions. In Fig. 14(a) the thyatron is fired just before the rf pulse arrives at the tube, causing complete reflection of the incident pulse and zero transmission past the tube. In Fig. 14(b) the thyatron is fired while the rf pulse is passing through the tube. As a result, half of the pulse is reflected and half is transmitted. Fig. 14(c) shows the rf hold-off characteristic of the tube. With the tube fired after the pulse has been transmitted past it, no breakdown of the pulse during transmission is seen to occur.

It should be noted, that to the best of our information, the peak powers switched by this tube (expressed as a fraction of the waveguide power capacity of air filled guide) are higher and the switching times shorter than any so far reported in the literature for this type of discharge. Furthermore, this tube has been operated so as to hold off almost 2 megawatts of peak power (at one microsecond pulse width) but switching action could not be initiated with the available grid trigger voltages. It is expected that a change in cathode-grid spacing (now being incorporated into a new experimental tube) will overcome this problem.

2. DC Triggered Microwave Spark Gap Switch

The problems that posed themselves in connection with this type of switching device were: (a) the design of a spark gap producing an intense, jitter-free, concentrated discharge in a localized region in the waveguide, (b) incorporating the gap in a suitable waveguide configuration so that the resulting "cold" losses (i. e., with gap not triggered) would be low, (c) finding an effective way of superimposing a high dc field on the rf field propagating through the gap without increasing the "cold" losses or reducing the rf hold-off, (d) keeping the "isolation" and "arc loss" at reasonable values. In addition, very short switching times were desired (less than 30 nanoseconds).

Out of a number of different attempts at solving the above problems there finally emerged a satisfactory switch structure (to be described shortly).

One of the earlier attempts is shown in Fig. 15. The switch consists of a short transmission cavity in half-height (swayback) waveguide with input and output coupling structures in the form of inductive irises, one of which contains the spark gap (Fig. 16). The difficulties with this configuration were: excessive insertion loss (about 1.4 db), excessive jitter due to a spray type of discharge having a large random component, and excessively long switching time. Some improvement was obtained by going to a different transmission cavity configuration as shown in Fig. 17. By use of movable plungers a better input VSWR was realized. This was accompanied by a reduction in arc loss

(to 0.2 db with switch triggered) but also by an increase in "cold" insertion loss to about 0.5-0.9 db, mostly because of the lengthened cavity and the additional losses of the movable plungers. The approximate pulse shape envelopes for this arrangement are shown in Fig. 18.

It was next decided to try the same gap configuration in conjunction with a short slot hybrid and one movable plunger, as shown in Fig. 19 to produce a phase shift type of switch - that is - one in which the position of a standing wave minimum is shifted by approximately a quarter wavelength when a discharge is initiated. (In this case, with the switch in the untriggered state, power is transmitted from port 1 to port 4 with little loss, while a triggered discharge causes most of the power to be reflected back to port 1.) A truncated cone spark gap configuration (Fig. 20a) in normal height waveguide was substituted for the previous type and gave improved results, but the peak power handling capacity (300 kw) was lower than had been hoped for.

The most successful spark gap (shown in Fig. 20b) gave distinctly improved results with respect to jitter, rf power hold-off, switching time, and arc loss.

The reason for the improved behavior is the existence of a common discharge path for the dc and microwave spark and the attainment of twice the former dc field strength in the gap. In the other configurations, because of the annular construction of the trigger electrode, the discharge path was not uniquely defined and the dc triggered microwave spark could jump across two generally different paths. One of these lay on the surface of a cone extending from the outer edge of the annular region surrounding the trigger electrode to the opposite electrode. The other preferred path extended directly across the gap between the two electrodes. By appreciably intensifying the dc field with the available voltage and locating the strengthened field directly across the intended microwave discharge path, faster switching times, and more intense and regular sparking was realized with consequent reduction in both jitter and arc loss.

The switch characteristics are summarized below:

peak of holdoff power	about one megawatt (independent of pulse width)
rf switching time	less than 10 nanoseconds (see Fig. 21)
"cold" insertion loss (unfired condition)	0.1 to 0.2 db
isolation (as defined in Fig. 22)	17 db*
arc loss (fired condition)	0.2 - 0.3 db (at rf levels above 30% of switch holdoff power capacity)

* This figure may be better in a dual spark arrangement.

The characteristics of the dc trigger are as follows:

pulse amplitude	10-15 kv
pulse shape	half sinusoid of 10-15 nanosecond duration
pulse rise time	about 5 nanoseconds

The dc trigger source was a specially designed unit built by Pulse Associates of Flushing, N. Y. It is capable of supplying a 35 kv output pulse across a high impedance but has not as yet been fully utilized since this requires pressurization of the spark gap. Construction of a pressurized switch is now under way which should permit switching of peak rf powers from 4-5 Mw.

Whereas the thyatron switch rf holdoff power decreases with increasing pulse width, the dc triggered microwave spark switch is not subject to this limitation. In addition, it possesses the following advantages:

- 1) it is simple to construct and relatively inexpensive to fabricate;
- 2) it can be physically rugged;
- 3) at moderate power levels it can be operated at the same pressure as the waveguide and pressure windows are therefore not required;
- 4) the electrodes, the only parts of the switch subject to wear, are inexpensive and readily replaced;
- 5) by pressurization and change of gas fill, the power handling capacity can be substantially increased and wear of electrodes possibly reduced;
- 6) by control of pressure, the switch can be used over a wide range of rf power levels at large pulse widths, if desired, with a minimum dc power consumed in the switching, since a small fraction of the rf power will supply the power to maintain the discharge.

IV. Interaction of High Microwave Fields with Metals

Prof. H. Farber, J. W. E. Griemsmann, M. Sucher

The aim of this study was to consider the interaction of high microwave fields with metals and to determine whether any effects (other than thermal) are produced by the microwave fields.

A resonant cavity is the optimum circuit element for achieving high-power densities in localized volumes and for maximum energy transfer to small metallic surfaces. Furthermore, any non-thermal response of the metal would probably be very small and the cavity, by becoming detuned, would enhance any small impedance change of the metal specimen and thus make this change readily observable.

Several cavity configurations were analyzed. One design objective was to have the electric field tangential to the surface of the test piece since electron bombardment (by multipactor or by gas discharges) of the metallic surface could be a major factor in heating or eroding the sample. The results of the analysis indicated that a coaxial cavity resonant in the H_{011} mode would be best suited for these studies. The construction of such a cavity with provisions for evacuation and replacement of the center conductor is shown in Fig. 23.

The ratio of inner to outer radius was chosen as 0.1 to obtain the maximum power transfer per unit area to the center conductor which is the test specimen. (See Fig. 24.) Low power microwave measurements gave the following cavity parameters:

- 1) Unloaded $Q \approx 10,000$
- 2) Tuning range 5.1 - 5.5 kmc
- 3) No interfering modes at 5.3 kmc within total tuning range
- 4) TE_{31} mode resonance possible at 5.5 kmc

Several center conductors of aluminum, copper and steel were prepared with wall thicknesses of 1/8 inch and 3/16 inch. In spite of numerous waveguide window failures, a successful measurement was made with an aluminum center conductor (3/16 inch wall thickness). The test conditions were as follows: the pressure in the cavity was maintained below 6×10^{-5} mm Hg by limiting the rate at which the microwave power was increased; the microwave power was pulsed at 830 pps, at a pulse width of 1.2 microseconds. The microwave circuit is shown in Fig. 25. The average incident microwave power was measured with a power meter and directional coupler, and the incident and reflected powers and the stored energy were monitored simultaneously on a Tektronix 551 oscilloscope. A typical oscillogram is shown in Fig. 26

The aluminum center conductor failed after 19 minutes exposure to an average incident power level of 250 watts. Approximately 20% of this power is dissipated in the center conductor while the remainder is lost to the cavity walls.

The aluminum conductor broke into two pieces. A photo-micrograph of one end is shown in Fig. 27.

After the experiment, the outer cavity wall was observed to possess a highly reflective coating of aluminum which had been evaporated from the center conductor. Since aluminum does not sublime, the surface of the center conductor must have been molten during the experiment.

When the power level was raised to 400 watts average input power, the aluminum was melted within 10-30 seconds. In fact, it was possible to resonate the cavity even when $3/8$ inch of the center conductor had melted and slowly separated into two parts.

A similar series of experiments was carried out using stainless steel center conductors. At power levels ranging from 75 watts to 400 watts input the temperature of the center conductor ranged from a very dull red to a bright yellow, corresponding to an optical temperature of 2000°F. These temperatures were attained within 30 seconds of the application of power. In all cases, the cavity was coated with a mixture of nickel and iron. At the higher power levels breakdown within the cavity was a problem. This resulted from the appreciable thermionic emission from the center conductor which, in association with the high microwave fields, gave rise to a multipactor discharge.

A series of measurements using cw power was then undertaken to determine whether any appreciable difference existed between the effect of cw and pulsed power. Special arrangements were made with the Sperry Electron Tube Division in Gainesville, Florida to use their high power cw tube facilities. The series of measurements with stainless steel was repeated and no appreciable difference was noted between the cw and the pulsed power tests. A few tests were made at atmospheric pressures and these gave similar results to the tests in vacuum except that 10-15% higher input powers were needed in the 200-400 watt range.

At power levels of 600-650 watts, 3-30 seconds were required to melt the stainless steel samples at the center. The melted regions ranged from $1/16$ inch to $1/4$ inch along the axial dimension.

These measurements indicated that the interaction of the high microwave fields with the metal center conductors resulted only in the heating of the center conductors and not in any field effects per se since nearly equal cw and pulsed powers were required to produce the same result.

It may be of interest to note that the fields on the center conductor were about 40 times as large as they would have been in free space for the same input power. Further, if we consider the cavity as a transformer for matching the impedance of the metal surface to free space, we can compare the power absorbed by the central region of the cold center conductor with that absorbed by a unit of surface uniformly illuminated by a plane wave in free space. Assuming the same available generator power for both cases, the ratio of the absorbed powers is 1000 to 1.

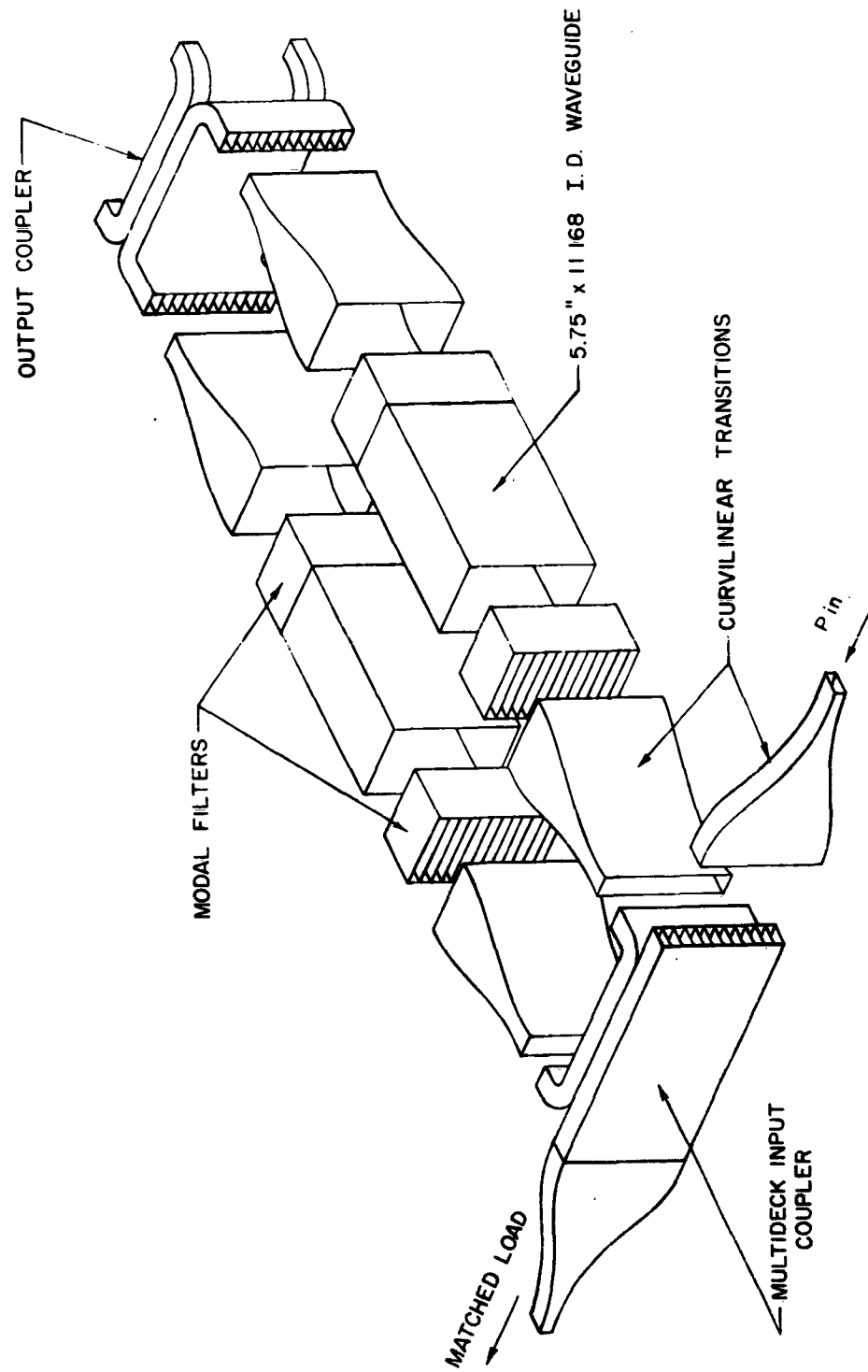
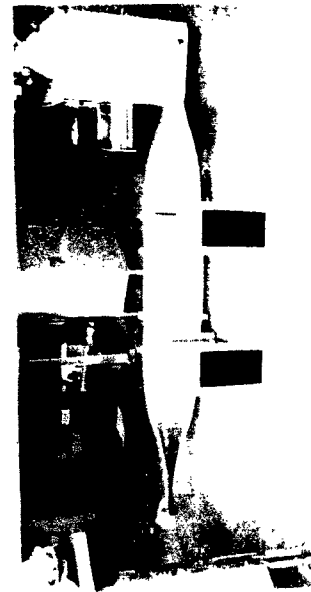
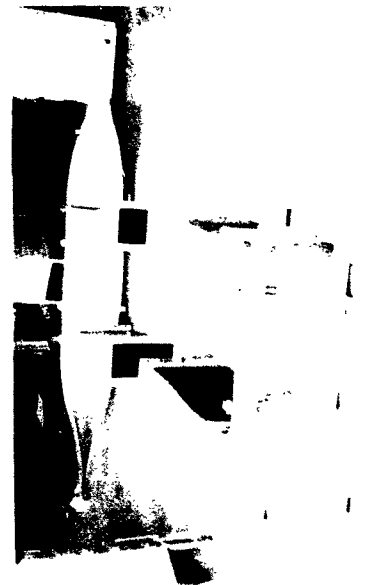


FIG. 1 OVERSIZED HIGH POWER C-BAND RESONANT RING



Multi-deck Feeding Coupler Assembly
Showing Flared Transitions



Partial Layout of Oversized
Traveling Wave Resonator

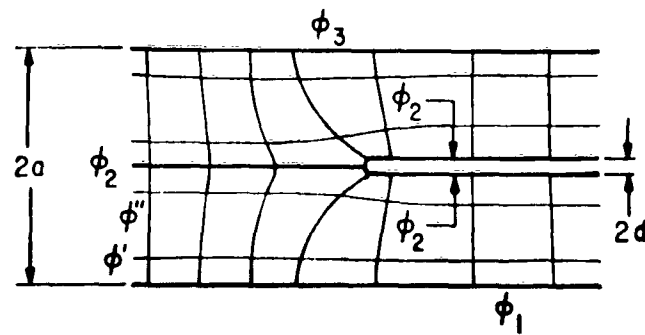


Multi-deck Sampling Coupler
Assembly

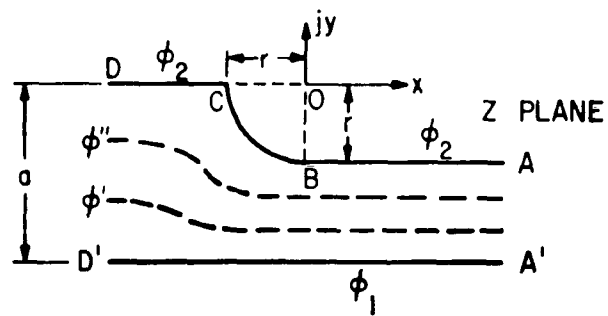


View of Multi-deck Feeding Coupler
Showing Coupling Hole Arrays

Fig. 2



(a)



(b)

Fig. 3 Plot of Electric Field and Equipotentials for Septated Waveguide

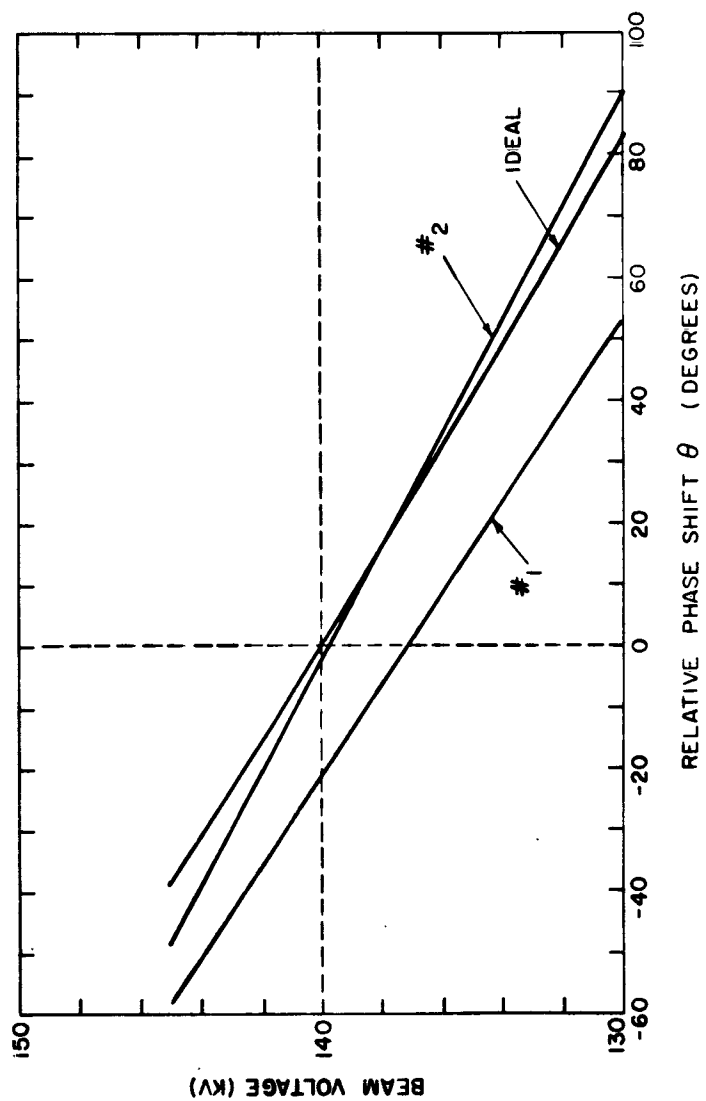


Fig. 4 Relation Between Beam Voltage on Klystron Amplifier and
Relative Phase Shift Between Input and Output Signals

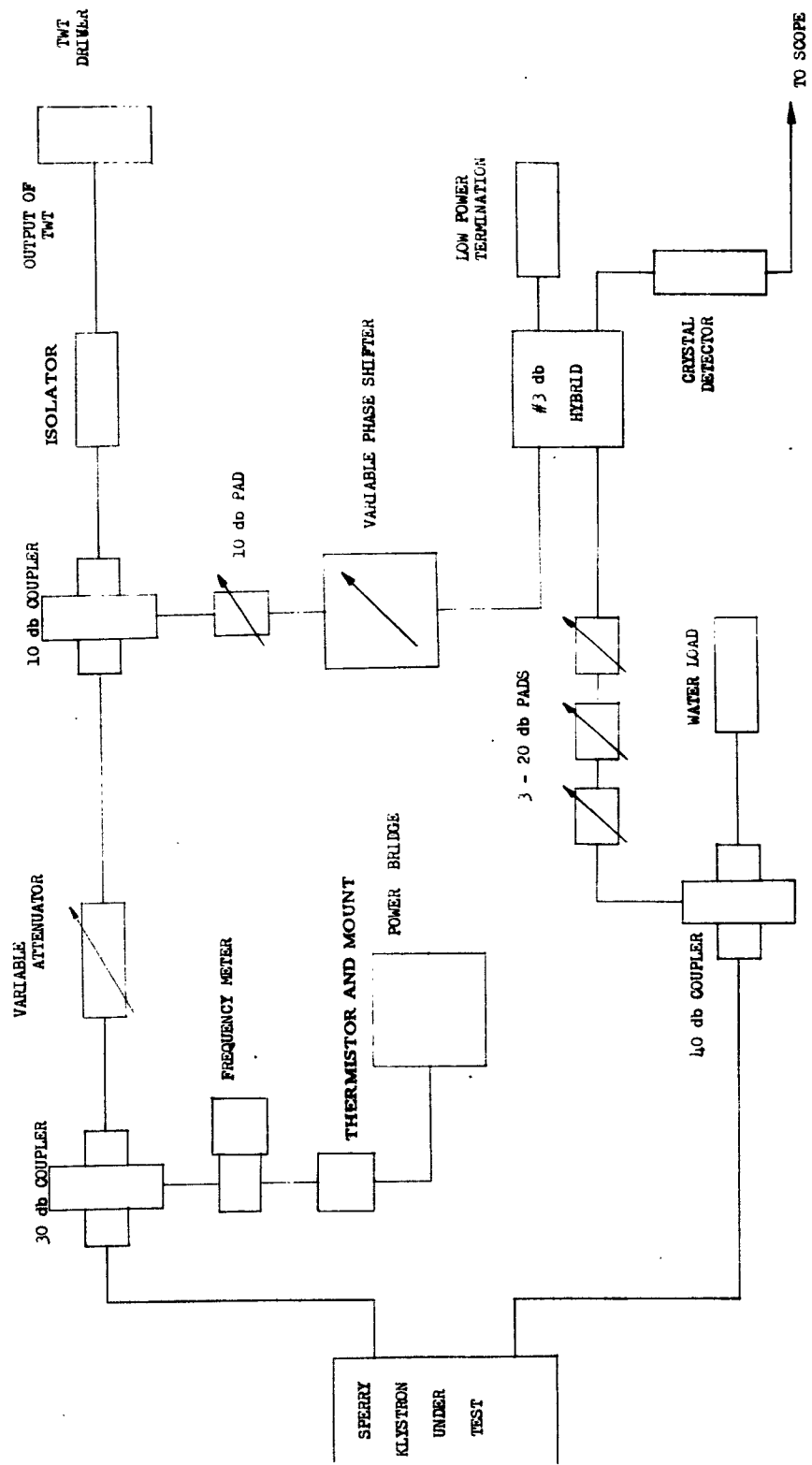


Fig. 5 Block Diagram of Setup for Measurement of Phase Shift as Function of Beam Voltage

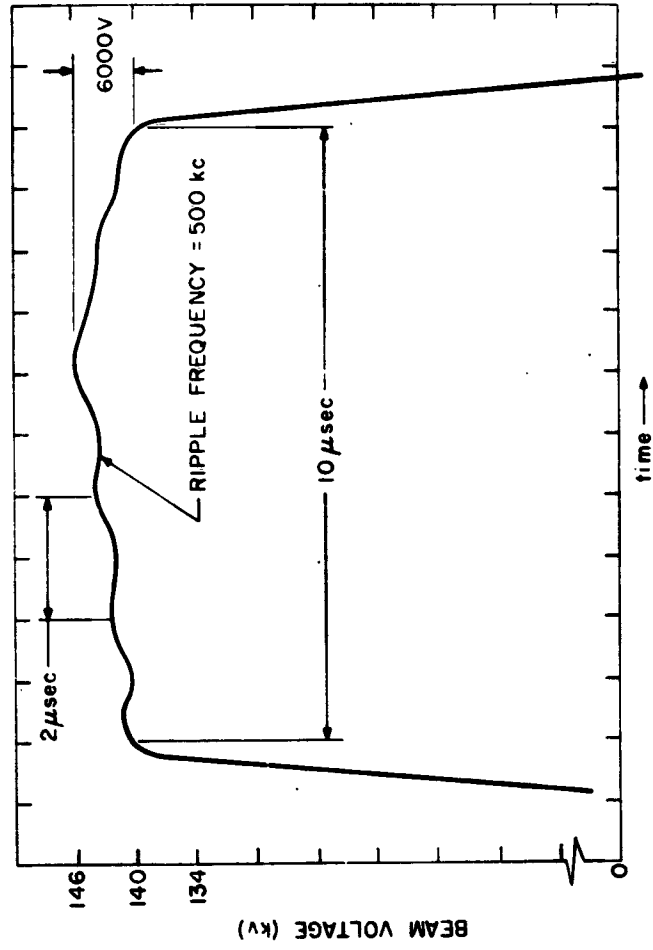
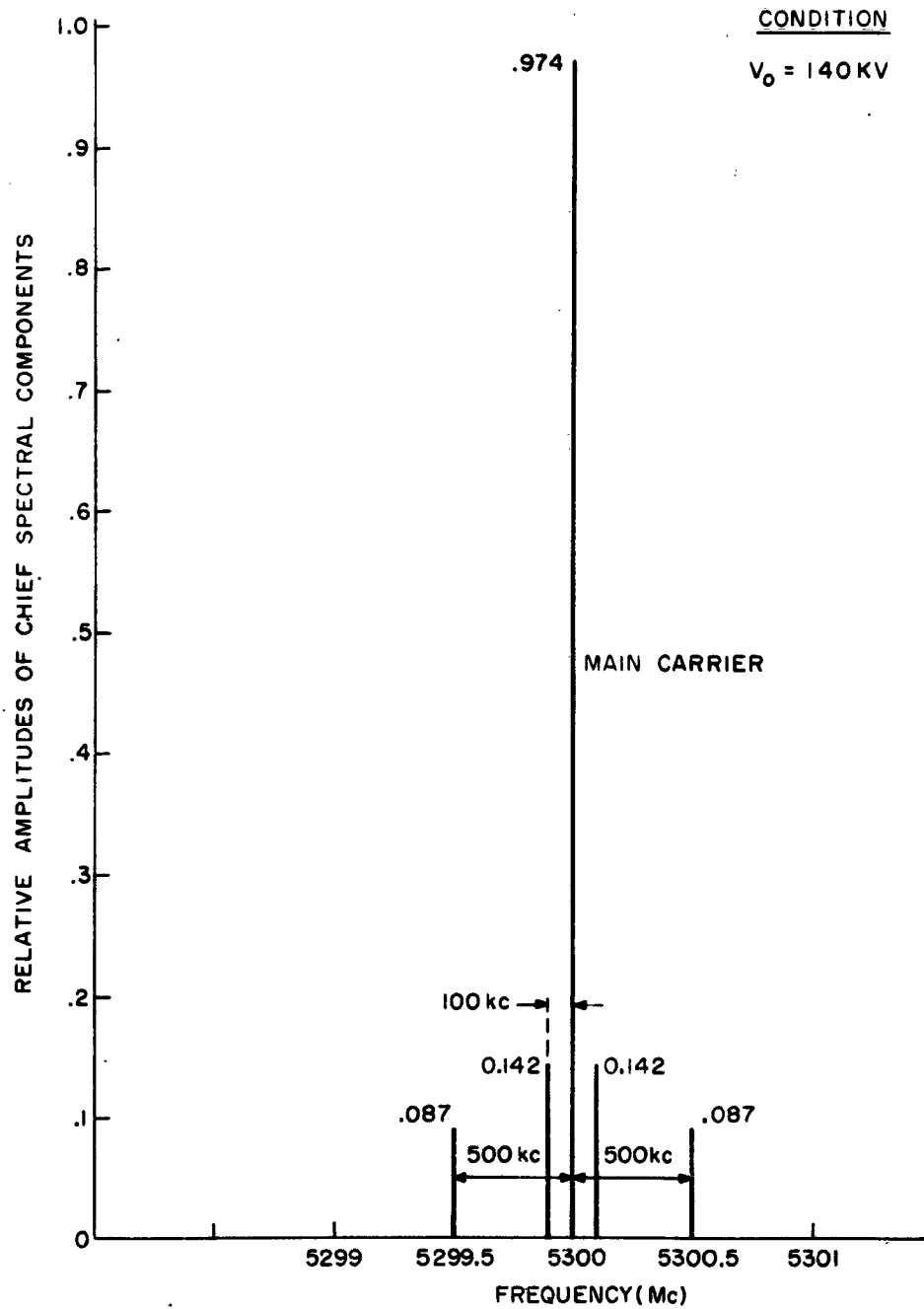


Fig. 6 Graphical Plot of Top of Beam Voltage Pulse

Fig. 7 Chief Spectral Components of Phase-Modulated Klystron Output Produced by Beam Voltage Pulse of Fig. 6



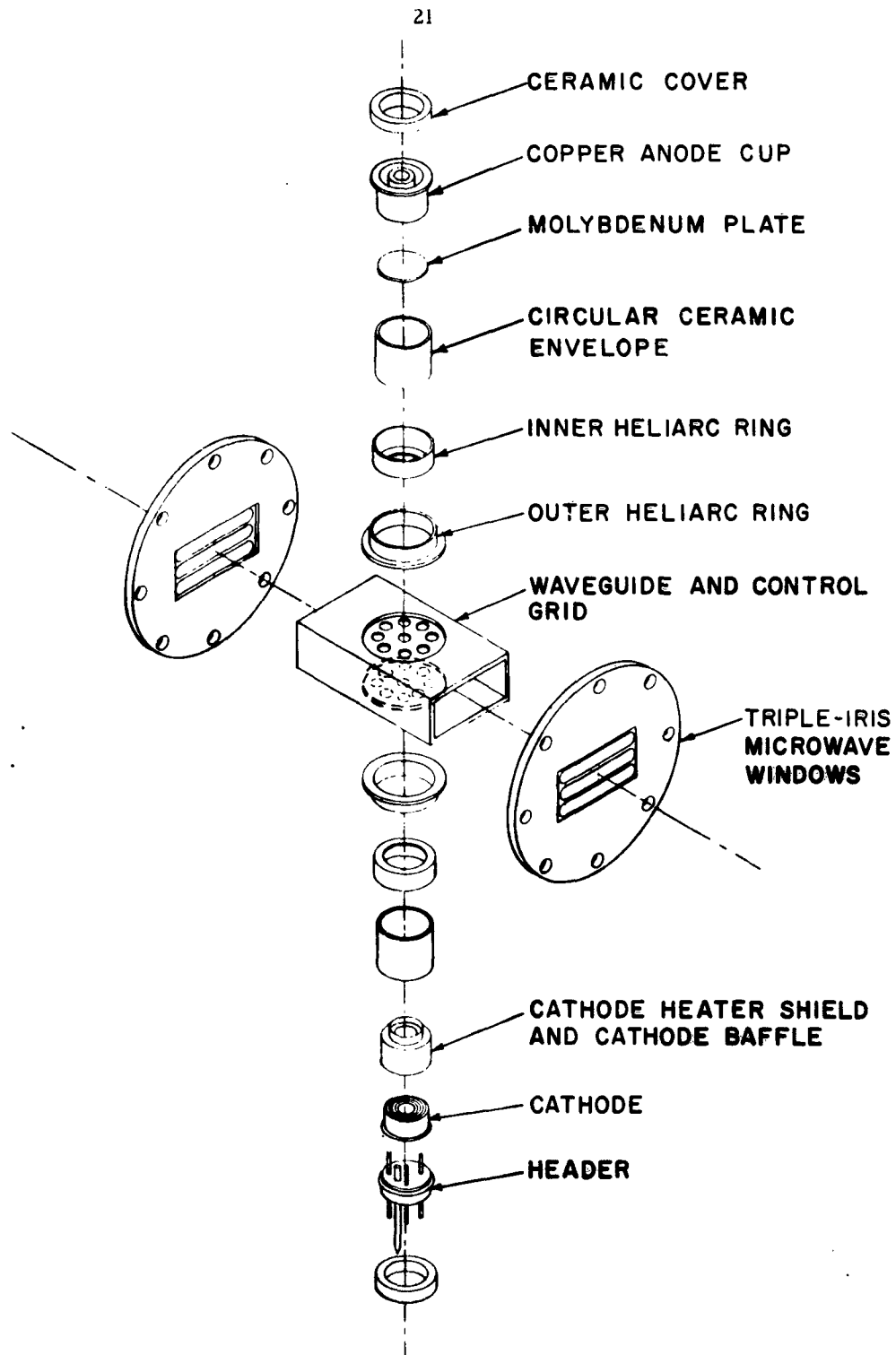


FIG. 8. EXPLODED VIEW - MICROWAVE LOW PRESSURE GAS DISCHARGE SWITCH TUBE

GC-40

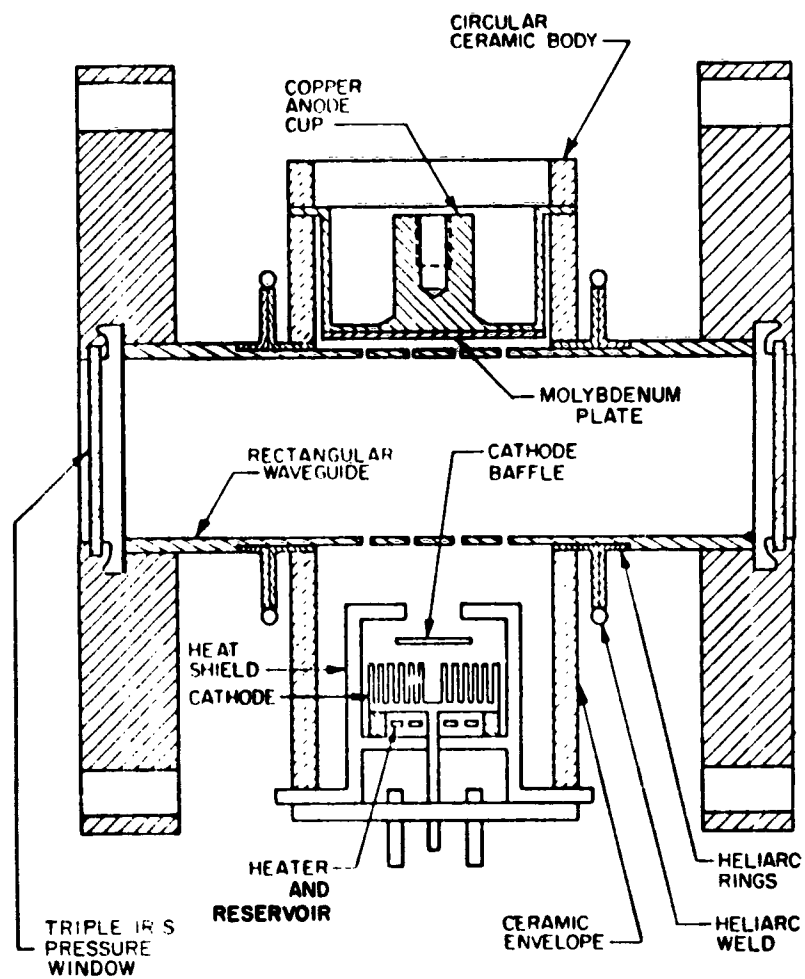


FIG. 9. LOW PRESSURE GAS SWITCH

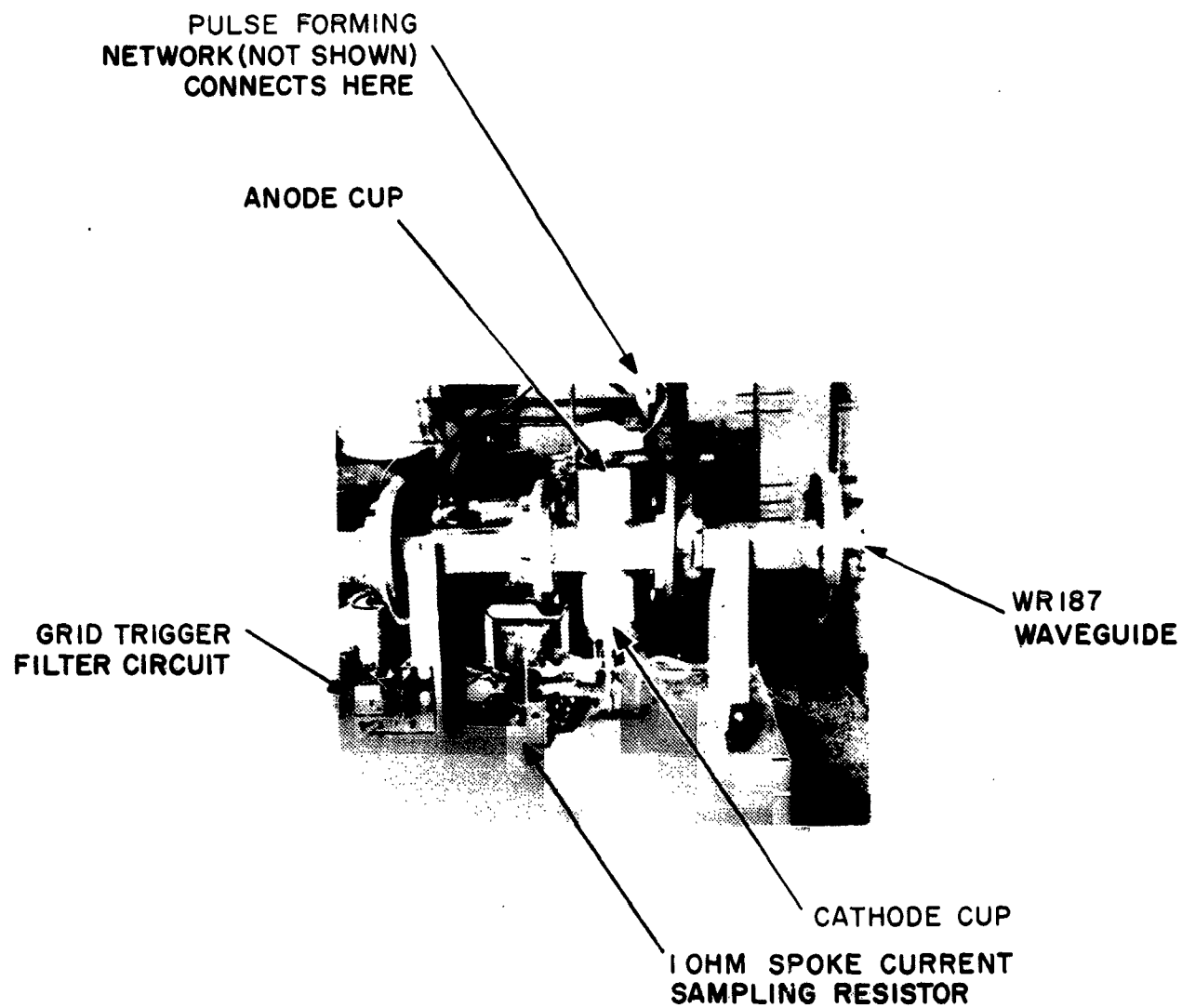
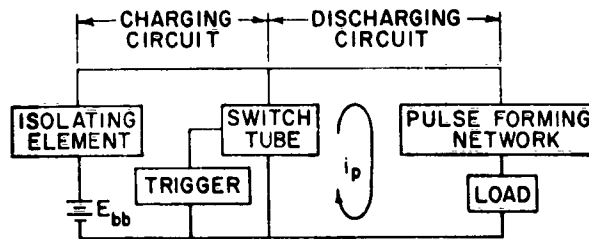


Fig. 10 Photograph of Waveguide Thyatron Switch



BLOCK DIAGRAM OF CHARGING AND DISCHARGING CIRCUITS

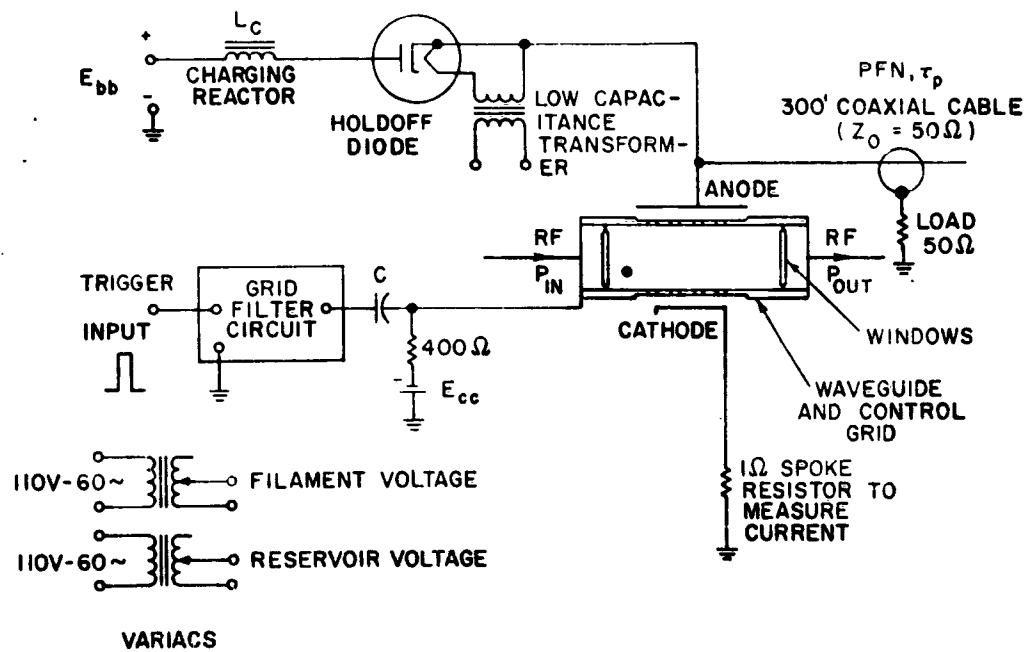


FIG. 11 SCHEMATIC OF MODULATOR

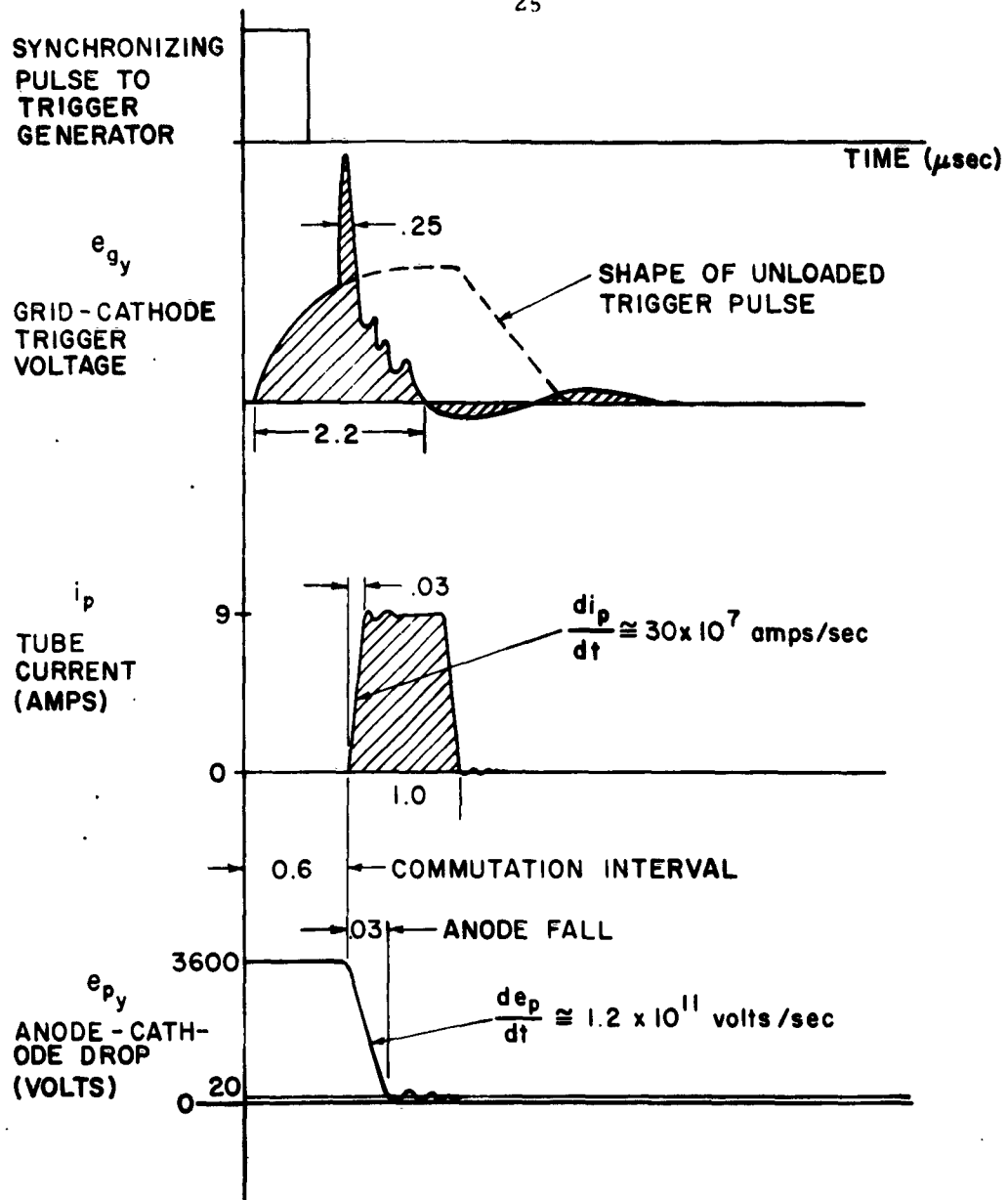


FIG.12. TYPICAL THYRATRON SWITCH TUBE
WAVEFORMS

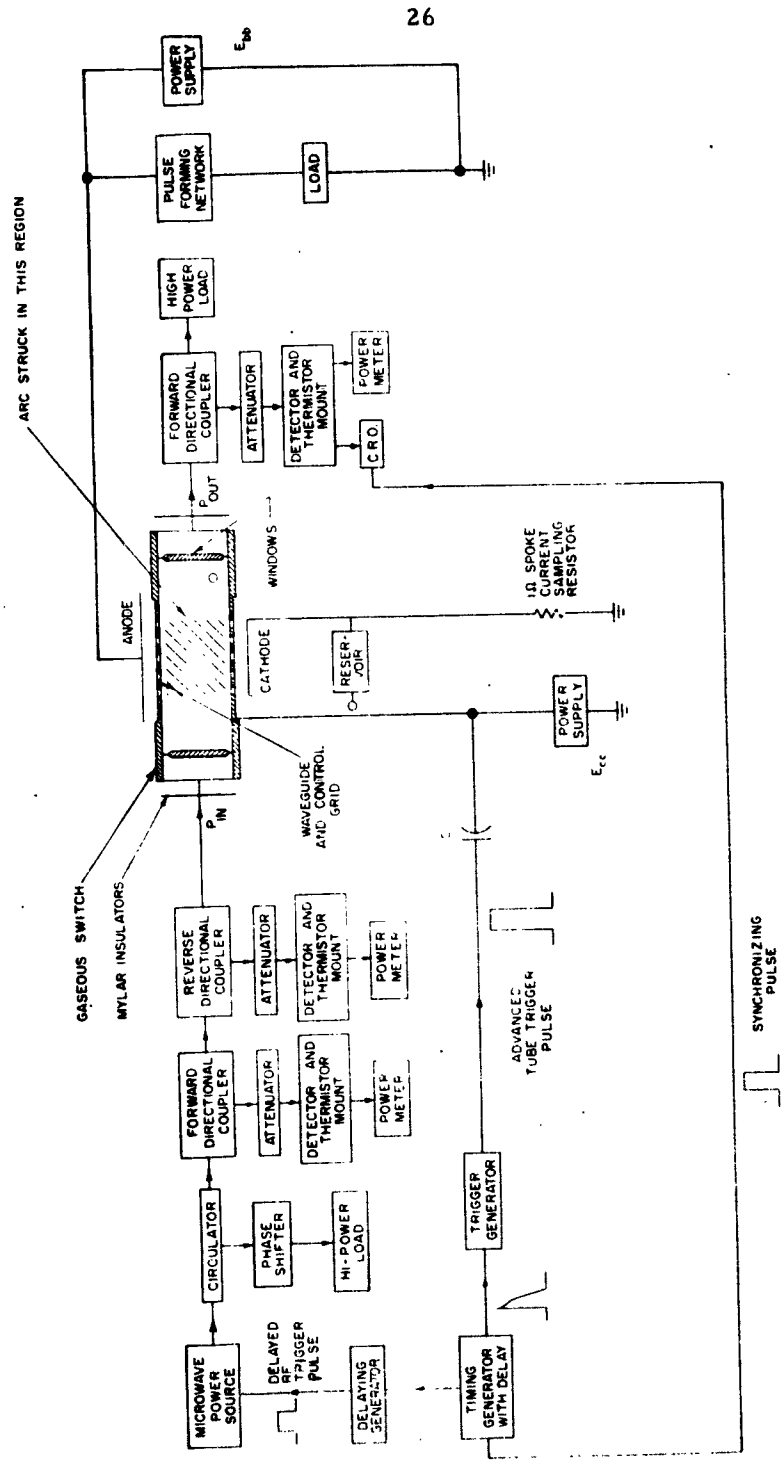


FIG. 13. HIGH POWER TEST FACILITY

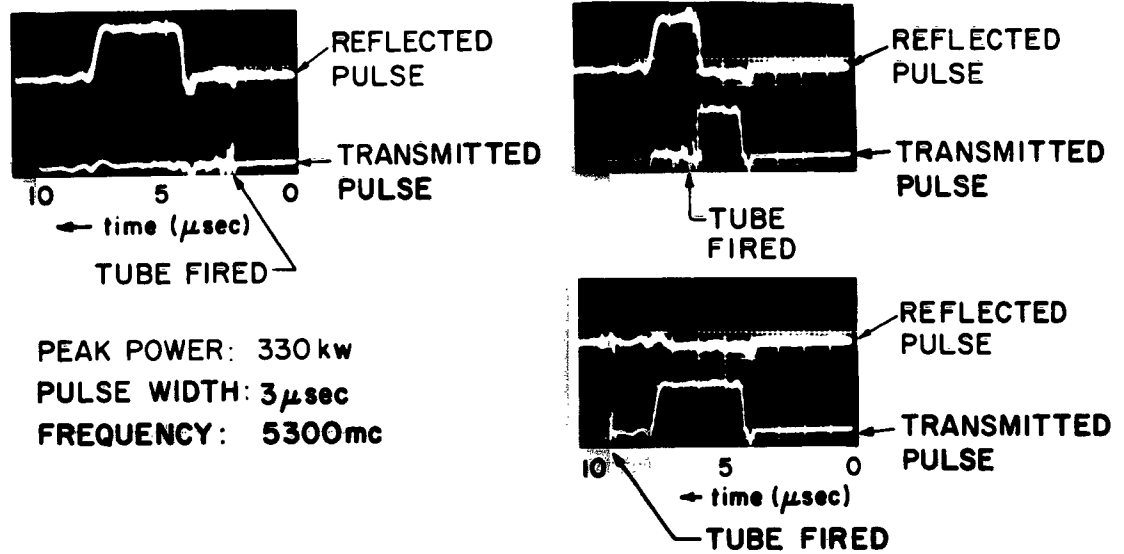


FIG. 14 OSCILLOGRAMS OF RF SWITCHING

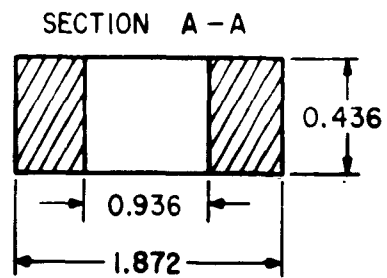
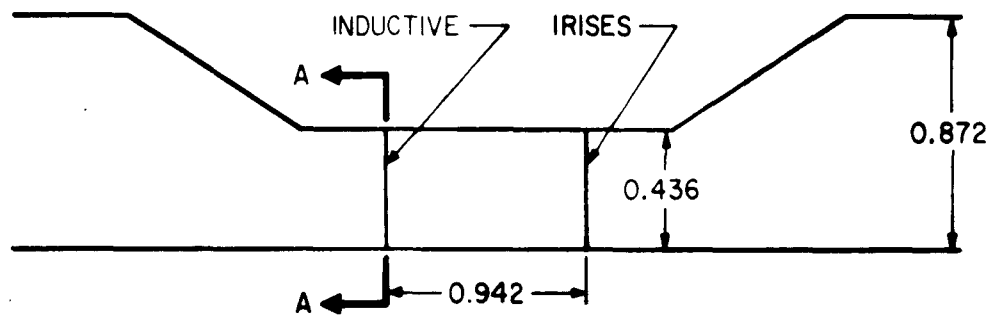
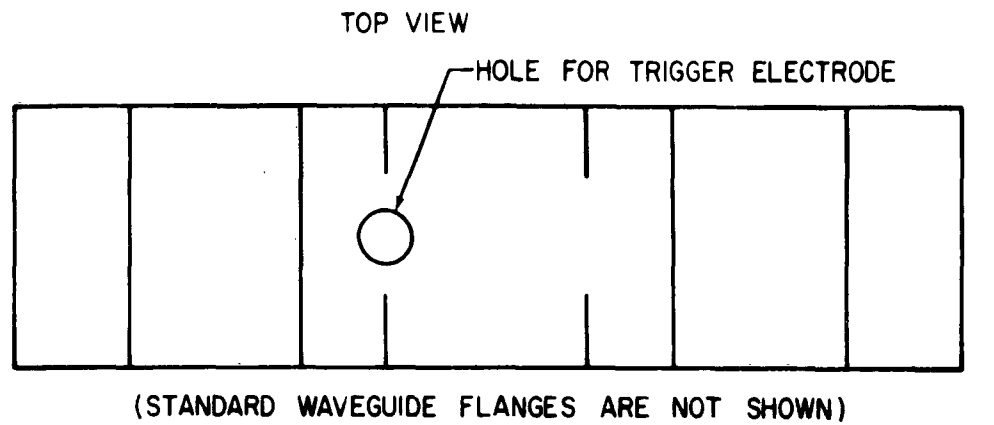


Fig. 15 Swayback Waveguide Spark Switch

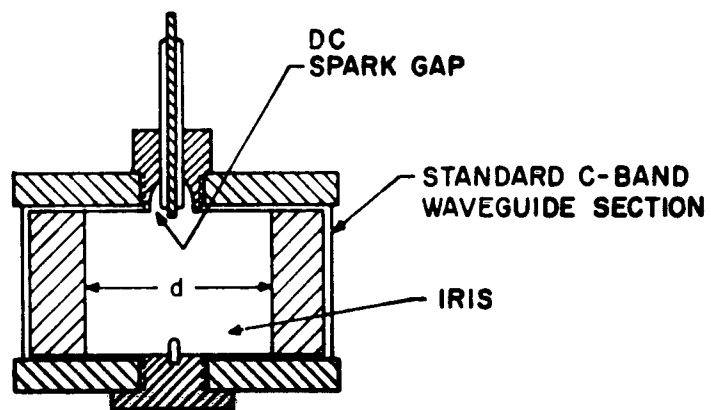


Fig. 16 Modified Spark Gap Configuration

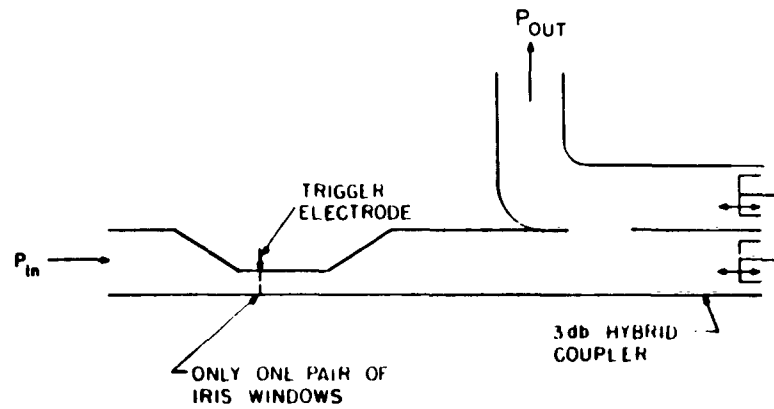


Fig. 17 Swayback Waveguide Spark Switch with Hybrid Coupler

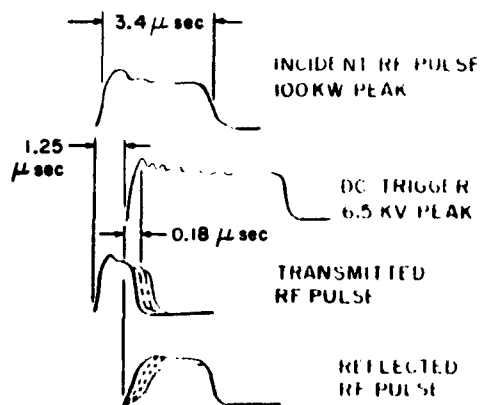
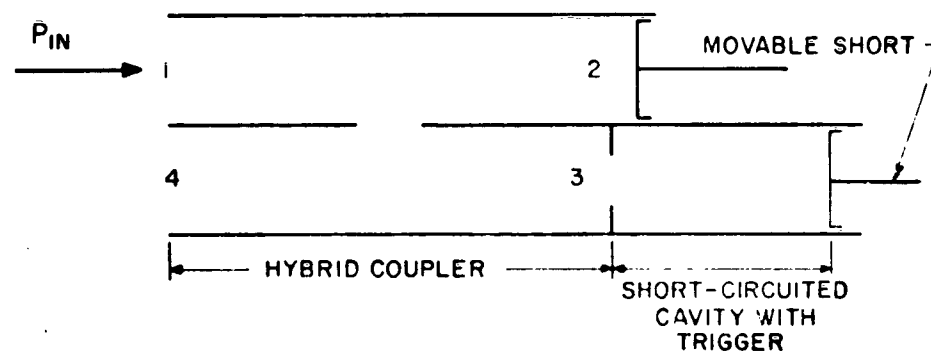
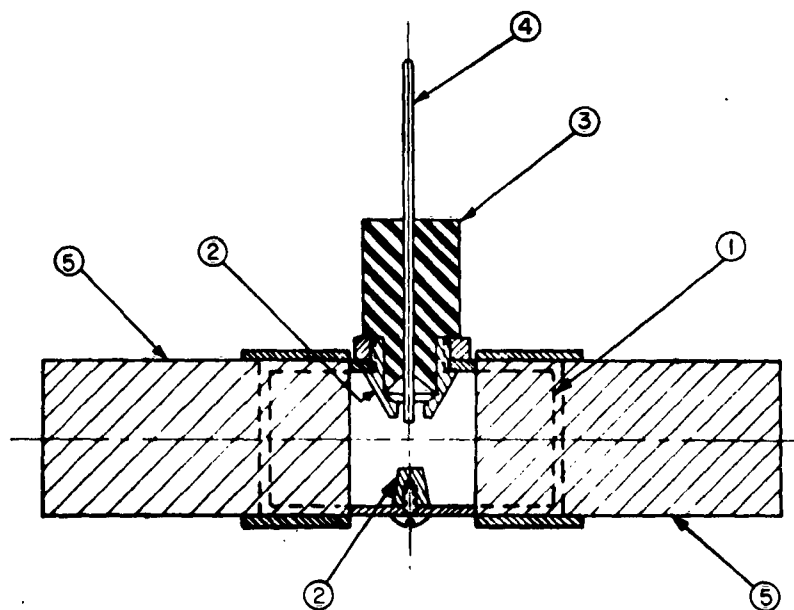


Fig. 18 Pulse Forms Shown on Oscilloscope



TEST SWITCHING ARRANGEMENT

FIG.19



- | | |
|---------------------------------|--------------------------------|
| ① CONVENTIONAL C-BAND WAVEGUIDE | ④ D-C TRIGGER ELECTRODE |
| ② TRUNCATED CONE ELECTRODES | ⑤ DIAPHRAGM TO ADJUST THE IRIS |
| ③ INSULATOR | |

**FIG. 20a TRUNCATED CONE MICROWAVE SPARK GAP
WITH IRIS**

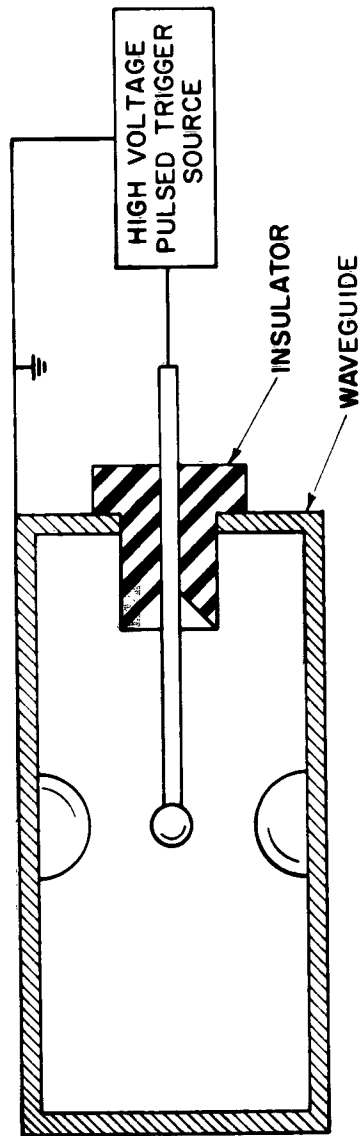
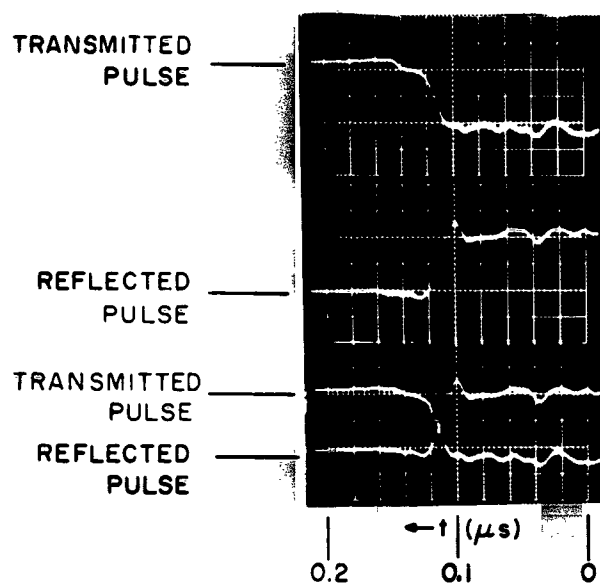


FIG.20b SCHEMATIC OF DC TRIGGERED MICROWAVE SPARK GAP



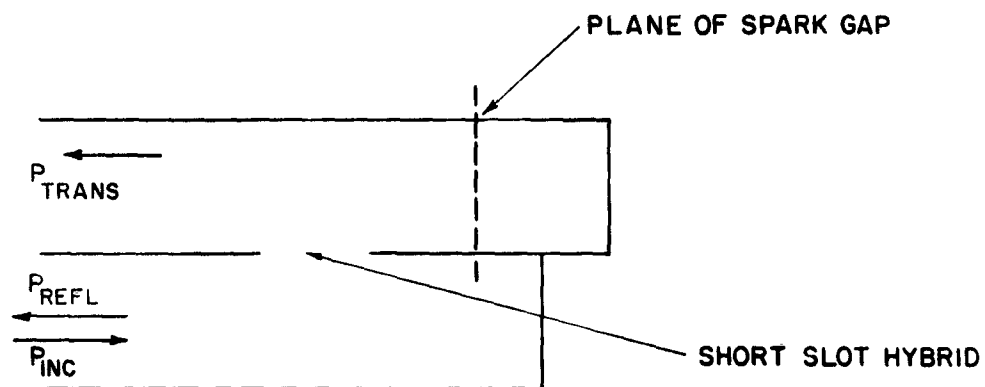
RF POWER: 600 kw

DC TRIGGER: 15 kv

SCOPE: TEKTRONIX 545 A

SWEEP TIME: 20 NANOSECONDS/cm

FIG.21 Oscillograms of switching by
dc triggered microwave spark



TERMINATING SHORTS ARE ARRANGED SO P_{trans} IS MAXIMUM IN ABSENCE OF SPARK. WHEN SPARK IS TRIGGERED P_{trans} DROPS AND P_{refl} RISES. ISOLATION IS DEFINED AS $10 \text{ LOG}(P_{\text{inc}}/P_{\text{trans}})$ AND ARC LOSS AS $10 \text{ LOG}(P_{\text{inc}}/P_{\text{refl}})$ FOR SWITCH IN TRIGGERED STATE.

FIG. 22. TEST ARRANGEMENT FOR DC TRIGGERED MICROWAVE SPARK

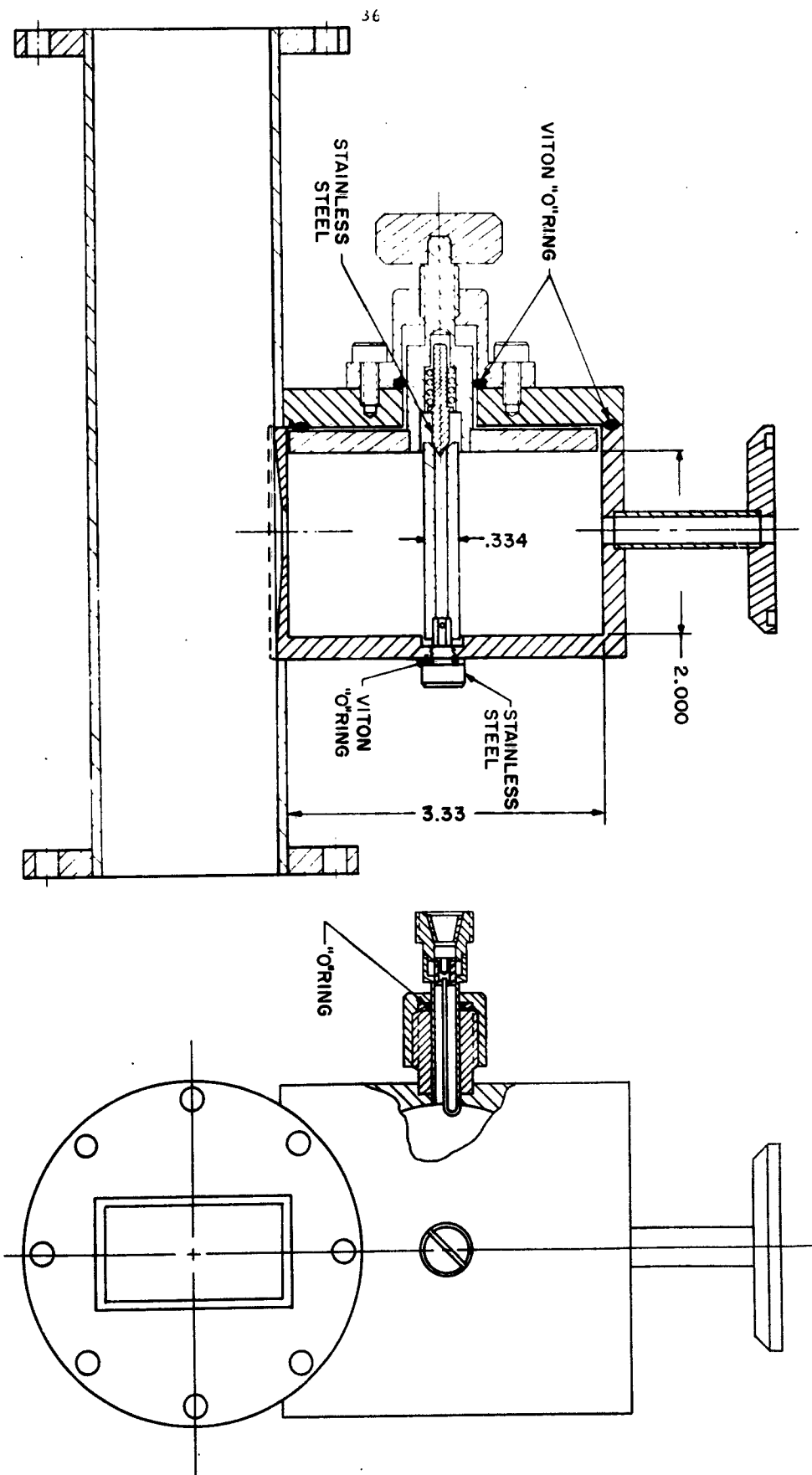


FIG.23. COAXIAL CAVITY

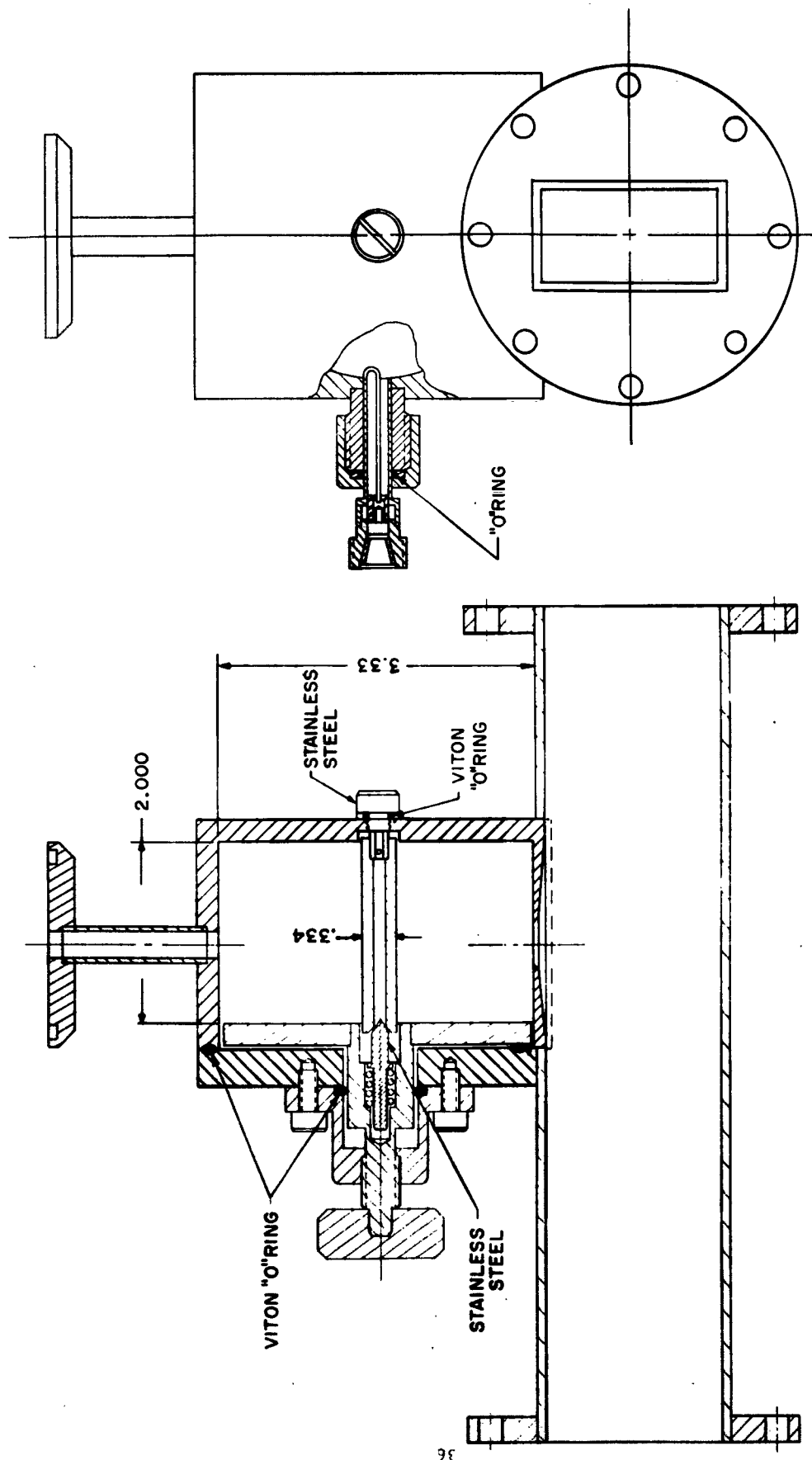
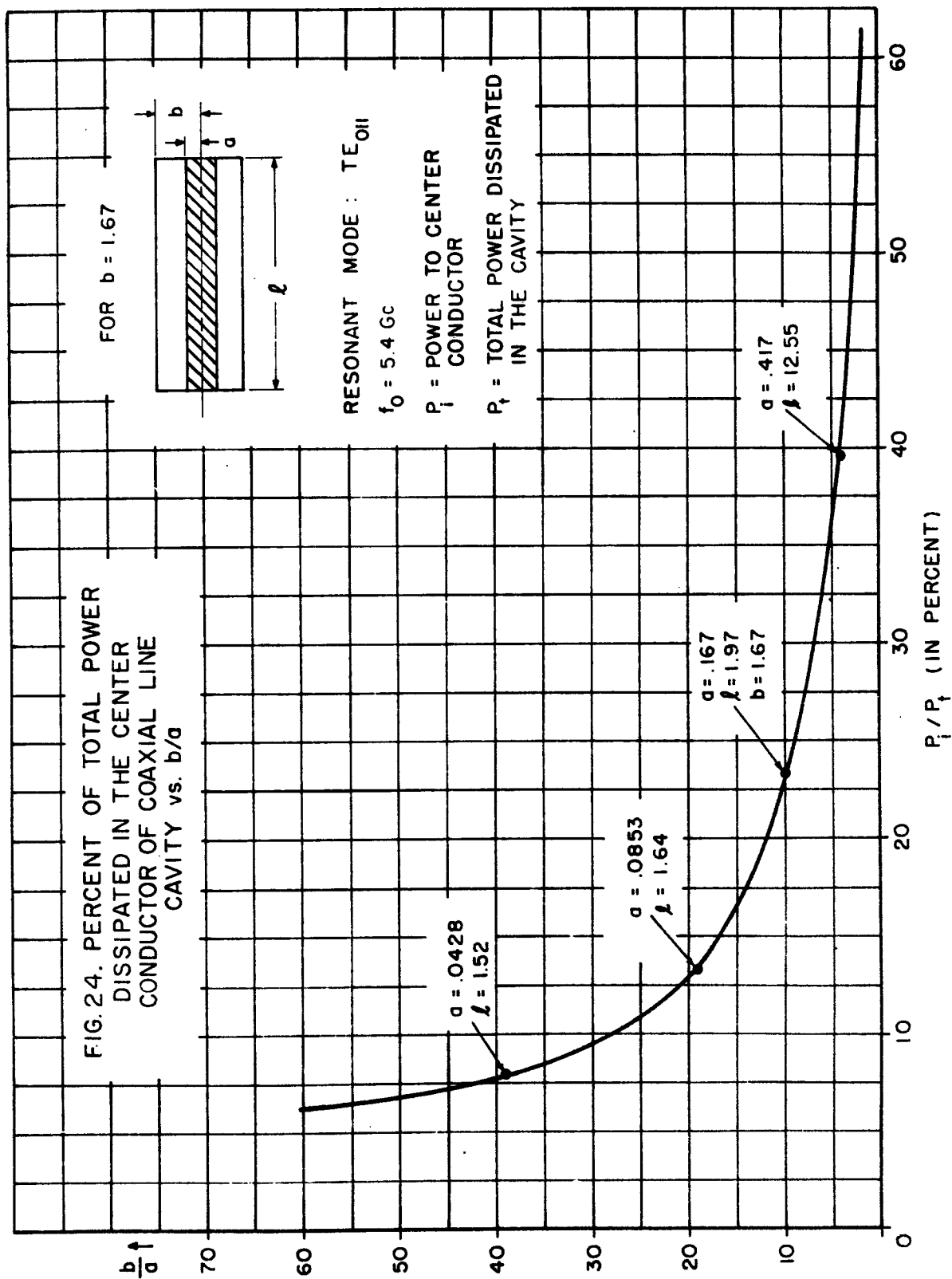


FIG.23. COAXIAL CAVITY



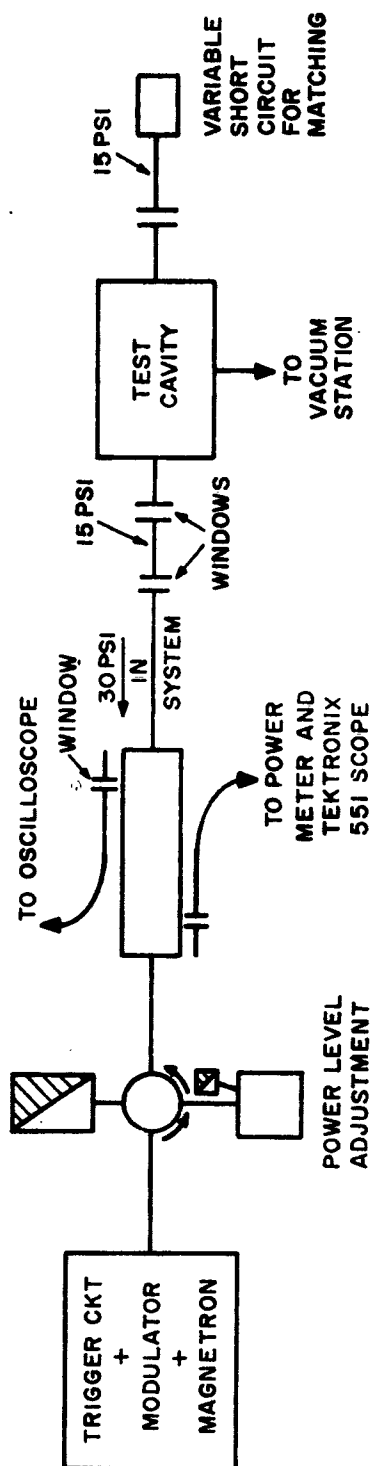
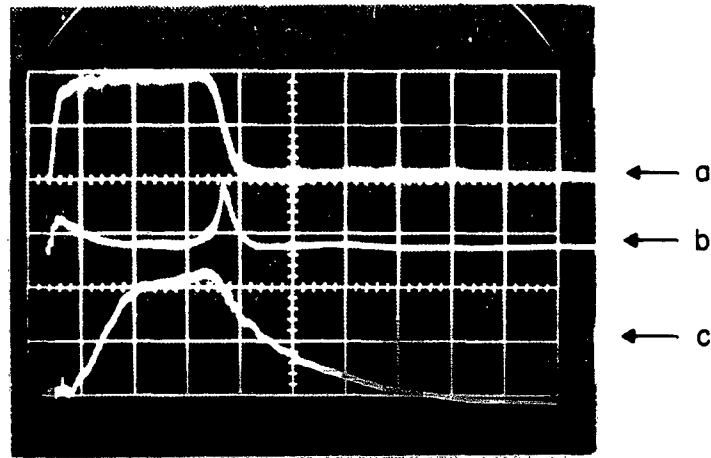


FIG.25. MICROWAVE TEST CIRCUIT



SWEEP = $0.5 \mu\text{sec/cm}$

POWER RELATIONSHIPS DURING TEST

- a: INCIDENT POWER
- b: REFLECTED POWER
- c: ENERGY STORED IN CAVITY

FIG. 26

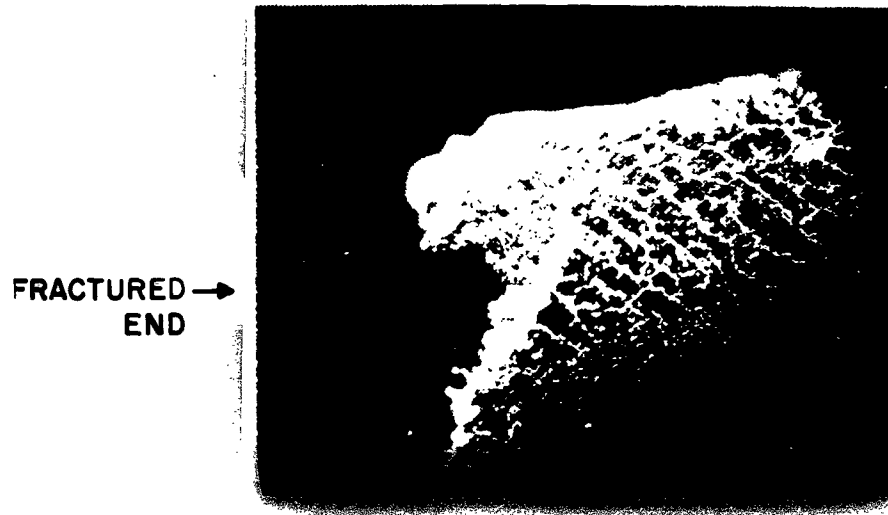


FIG.27. FRACTURE OF ALUMINUM CENTER CONDUCTOR
(SURFACE SHOWS SIGNS OF HAVING BEEN MOLTEN)

DISTRIBUTION LIST FOR CONTRACT REPORTS

RADC (RALTM ATTN: Mr. Vannicola) Griffiss AFB, NY	3	AFSC (SCSE) Andrews AFB Washington 25, DC	1
RADC (RAAPT) Griffiss AFB, NY	1	Commanding General US Army Electronic Proving Ground ATTN: Technical Documents Lib. Ft. Huachuca, Ariz.	1
RADC (RAALD) Griffiss AFB, NY	1		
GEEIA (ROZMCAT) Griffiss AFB, NY	1	AFPR General Electric Company Lockland Branch POBox 91 Cincinnati 15, Ohio	1
RADC (RAIS, ATTN: Mr. Malloy) Griffiss AFB, NY	1		
US Army Electronics R & D Labs. Liaison Officer RADC Griffiss AFB, NY	1	Chief, Bureau of Ships ATTN: Code 312 Dept. of the Navy Washington 25, DC	1
AUL (3T) Maxwell AFB, Ala.	1	Office of the Chief Signal Officer ATTN: SIGRD Dept. of the Army Washington 25, DC	1
ASD (ASAPRD) Wright-Patterson AFB, Ohio	1	Dielectric Products Company ATTN: Dr. Charles Brown Raymond, Maine	1
Chief Naval Research Lab. ATTN: Code 2027 Washington 25, DC	1	Armour Research Foundation of Illinois Institute of Technology ATTN: J. E. McManus Chicago 15, Illinois	1
Air Force Field Representative Naval Research Lab. ATTN: Code 1010 Washington 25, DC	1		
Commanding Officer US Army Electronics R & D Labs. ATTN: SELRA/SL-ADT Ft. Monmouth, NJ	1	Kane Engineering Corp. ATTN: Dr. Kane Palo Alto, California	1
DDC (TISIA-2) Arlington Hall Station Arlington 12, Va.	10	Sperry Gyroscope Co. ATTN: Lenard Swern Lake Success, New York	1
		RADC (RALTP/Mr. Quinn) Griffiss AFB, NY	1

RADC (RALSP/Mr. J. Cameron) Griffiss AFB, NY	1	Scientific Engineering Institute ATTN: Mr. Daniel Schwarzkoph 140 Fourth Avenue Waltham, Mass.	1
RADC (RALS/Mr. Dovydaitis) Griffiss AFB, NY	1		
		Cornell Aeronautical Laboratory ATTN: Mr. Beitz Buffalo, NY	1
RADC (RALCD/Mr. Koegler) Griffiss AFB, NY	1		
Advisory Group on Electronic Devices Working Group on Microwave Devices ATTN: Mr. W. Kramer 346 Broadway New York, New York	2	General Engineering Lab. ATTN: George E. Feiker Schenectady, NY	1
Commanding Officer USASRDL ATTN: SIGRA/SL-PEE/Mr. Lipetz Fort Monmouth, NJ	1	Sperry Gyroscope Co. ATTN: Frank Liebert Mail Sta. D-40 Great Neck, LI, NY	1
Bureau of Ships - 691B2C Electronics Division Room 3329 Main Navy Building ATTN: Mr. Leo V. Gumina Washington 25, DC	1	Lincoln Lab. ATTN: Victor Pineo Lexington, Mass.	1
Airborne Instruments Laboratory ATTN: Mr. Avery Deer Park, LI, NY	1	Microwave Associates, Inc. ATTN: Meyer Gilden Burlington, Mass.	1
General Electric Co. Heavy Military Electronics Dept. ATTN: Dr. Joseph C. Almasi Syracuse, NY	1		
ESD ATTN: S. Herskovitz LG Hanscom Field Bedford, Mass.	1		